Coplanar stripline (CPS) emitter and transceiver microprobes for ultra-high bandwidth on-chip Terahertz measurements

C. Matheisen, M. Nagel, S. Sawallich
Protemics GmbH, Otto-Blumenthal-Str. 25, 52074 Aachen, Germany

***Abstract* — A novel THz emitter and transceiver for on-chip failure location and waveguide inspection is introduced. Based on a flexible PET cantilever it features a CPS waveguide for wear-free capacitive coupling to devices under test (DUTs). Embedded LT-GaAs photoconductive switches allow for ultra-high bandwidth THz pulse generation and detection which is demonstrated in exemplary measurements on CPS structures featuring different types of discontinuities. After coupling to the DUT pulse rise-times as short as 0.6 ps are achieved.**

I. INTRODUCTION

PLANAR THz waveguide structures are becoming increasingly important for integrated applications such as broadband chip-to-chip communication or on-chip sensing. The advantage of guided and confined wave transmission is exploited for sensor- and biomedical applications in order to achieve high sensitivity at minute sample volumes like i.e. in combination with hybrid microfluidic structures [1]. In addition, the waveguide development itself is a topic of great current interest [2-4]. So far, the use and analysis of THz waveguide structures has been difficult since a versatile way of injecting and detecting ultra-high bandwidth signals is lacking. At lower mm-wave frequencies, passive microprobes are routinely applied to connect a DUT to a signal source and detector. However due to the strong bandwidth limitation in cables and the needles itself this is not applicable as broadband solution in the higher THz range. Besides this, needles rely on a mechanical DC-contact and hence often cause unavoidable damage to the surface of the DUT.

In order to enable broadband (>1THz) on-chip THz signal transmission photoconductive (PC) emitter and detector components have been directly integrated into chip-based transmission lines [5]. This approach has also been used for sensing applications [6][7]. However, the costs for the fabrication of the sensing chips are very high – considering such a chip can be used only once. Furthermore, device-to-device tolerances of emitters and detectors may limit the comparability of measurements. Therefore, to serve the increasing need for high bandwidth THz on-chip measurements for failure location, device testing and sensing applications, the decoupling of emitter and detector components in terms of active ultrafast microprobes also capable of contactless operation [8] has recently found increasing interest – also for frequency-domain operation [9].

In this work, novel emitter and transceiver microprobes based on a flexible cantilever are introduced. The microprobes are capable of injecting and detecting ultra-high bandwidth THz pulses into CPS waveguides. The performance of the microprobes are demonstrated at a set of CPS structures featuring different passive devices. Near-field measurement data revealing field distributions of mode profiles and propagation dynamics are presented. Thanks to a record breaking short rise-time of 0.6 ps for chip-injected pulses (which is more than an order of magnitude shorter than current commercially available probes) deep-sub-wavelength structural differences below 20 µm length are resolvable in different faults using numerical signal analysis.

II. RESULTS

The emitter and transceiver microprobes are based on a 175 µm thick flexible PET cantilever featuring a CPS matched to the waveguide geometry of the DUT with a line width of 50 µm and a line spacing of 30 µm. A LT-GaAs-based emitter with a 2.5 µm-gap PC switch is embedded into the microprobe CPS in 1 mm distance from the coupling end. The microprobe is placed on the sample device in flip-chip configuration for a broadband coupling to the CPS under test as shown in Fig. 1(a).

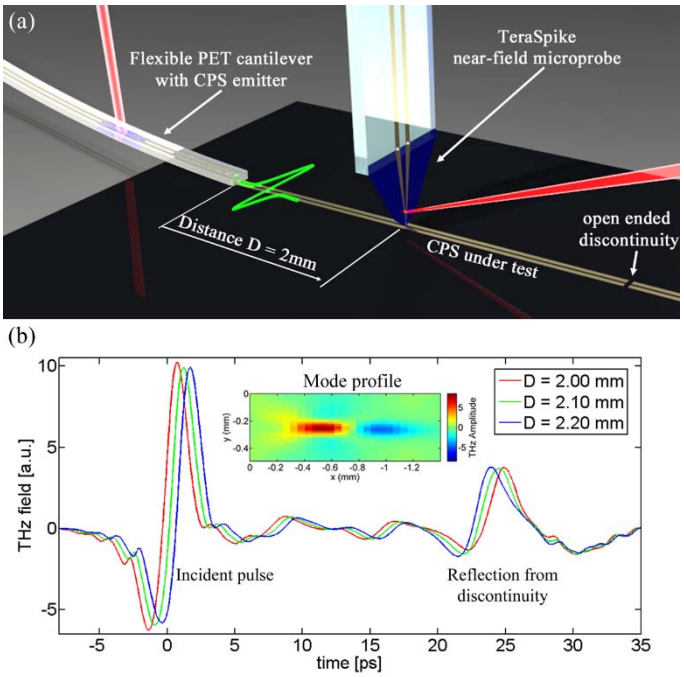

Fig. 1. (a): Schematic sketch of the experimental set-up around the CPS under test. **(b)**: Recorded THz time-transients in this set-up at different distances to emitter and discontinuity respectively. Inset: Spatially resolved measurement of the mode profile on the CPS under test.

Using a femtosecond laser with 80 MHz repetition rate, 780 nm central wavelength and <100 fs pulse duration a broadband THz-pulse is generated and guided along the microprobe CPS. For the investigation of the emitter and coupling performance a separate photoconductive near-field probe is placed in ca. 5-10 µm distance above the DUT's stripline and the transversal electric field distribution of the propagating CPS mode is measured. The spatially resolved image, shown in the inset in Fig. 1(b) reveals that the regular

odd mode is dominantly excited which is characterized by strong field confinement between the striplines. An exemplary series of time-transients (Fig. 1(b)) shows incident and reflected pulses from an open-ended CPS discontinuity at different detector distances. In this case, the discontinuity is an interruption of both CPS lines as shown in Fig. 1(a).

In a first set of experiments, the detector position is varied along the CPS and transient signals covering the initial pulse transmission between emitter and detector as well as reflections from DUT- or probe-internal discontinuities are recorded. From the analysis of this data the complex propagation constants of the sample CPS can be determined. Additionally, by monitoring the shift of the signal contributions it is possible to distinguish unambiguously between the signal features originating from the DUT and the ones from the emitter microprobe itself. The time-transients plotted in Fig. 1(b) exhibit that the reflection from the open-end discontinuity is visible for approx. $t > 17$ ps since only in this later time range the signal is shifting towards the initial pulse as the distance D to the emitter increases. Weaker oscillations in between the initial pulse and $t = 17$ ps are hence caused by the emitter and the capacitive coupling to the DUT.

The transients also indicate that the damping of the CPS waveguide on PET substrate is relatively small. Therefore, it is important to take account of reflections possibly generated within the emitter microprobe itself. Within the microprobes introduced in this work, the suppression of these parasitic reflections is realized by an absorbing structure integrated into the CPS lines. The absorbing structure makes use of a resistive metallic layer that results in a highly increased damping of the guided THz signal. It is placed between the emitter and the external probe connectors and includes a tapered transition towards the direction of incident THz pulses to prohibit reflections caused by an abrupt impedance mismatch. Therefore, also long time-transients are free of larger parasitic disturbing reflections and allow for background-free analysis of the DUT.

To demonstrate this, Fig. 2(b) shows a set of longer time-transients of a more complex DUT. The CPS under test has a gap in one of the two lines followed by a short-circuit in 100 µm distance. In addition, it has an open-end after another 5 mm (see Fig. 2(a)). Emitter and detector are placed as shown in Fig. 1(a) and hence measure the device in reflection in a transceiver-like scheme. Again, two time-transients have been acquired at different positions on the DUT. To better visualize the reflections both time-transients have been shifted in time in reference to the initial incident pulse. Clearly, only the reflections from the discontinuities show a temporal difference from the remaining signal.

In comparison to the time-transients in Fig. 1 obtained at an open-end, the pulse shape for the first reflected signal in Fig. 2(b) originating from the gap/short failure structure looks significantly different. Thanks to the 0.6-ps-short rise time of the incident pulse and the resulting high transmitted bandwidth of up to 2.5 THz (see Fig. 2(c)) it is easy to distinguish between the two different failures even by eye. While the single gap causes a reflection of the incident pulse with same sign and similar shape but reduced amplitude the short causes a reflection with inverted sign. Hence, the second positive peak within the reflection can be addressed to the short discontinuity.

It has been shown earlier [8] that even with 1.1 ps rise times localization accuracies of better than 1 µm can be achieved because of the quasi jitter-free optical detection scheme which is also applied in this work. At least the same accuracy can be expected in this case. The maximum visible distance to fault (DTF) is limited by the system´s signal-to-noise ratio (SNR) and the transmission loss of the DUT. In our case, the reflection from the very end of the CPS can be clearly identified although the pulse propagates already over a relatively long distance of 1.6 cm and passes twice the discontinuity in between. The reflection from the open-end still has a rise time of 1.5 ps. On the one hand this highlights the capability for spectroscopic investigations of planar on-chip structures. On the other hand it demonstrates the strong potential for on-chip fault detection and analysis. The estimated maximum DTF calculated from our data is 4.2 cm (assuming a remaining SNR = 6).

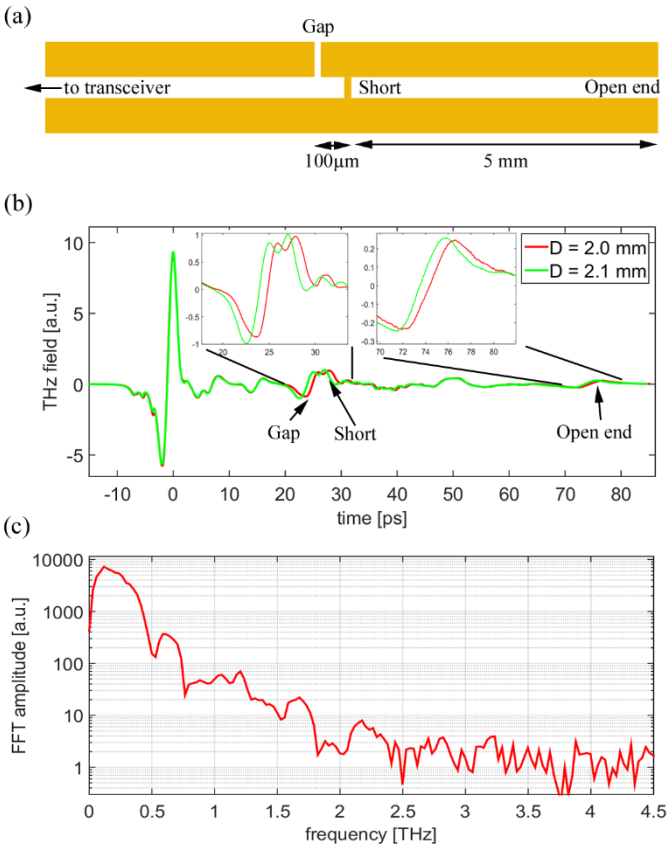

Fig. 2. (a): Schematic sketch of the combined gap/short defect structure with 100µm distance and an open end at the very end. **(b)**: Recorded THz time-transients in reflection on this DUT at two different distances. **(c):** Spectrum of the incident pulse on the DUT.

The ability to easily swap between DUTs without changing emitter or detector as a requirement for doing consecutive measurements at high throughput and good repeatability is shown in the following. High bandwidth and short rise-time are essential to enable the identification of singular structures. The minimal distance d_{min} of two discontinuities required for their discrimination is approximately given by

$d_{min} = \tau_{rise} \cdot c/4\sqrt{\varepsilon_{r,eff}}$ where τ_{rise} is the rise-time of the pulse, c the speed of light and $\varepsilon_{r,eff}$ the relative effective permittivity of the DUT [10]. For the configuration demonstrated here, the calculated d_{min} is as low as 35 µm, whereas in comparison an alternative system using also fs-laser driven photo-switches for pulse generation but narrow-band waveguides for pulse-to-DUT signal transmission (leading to 5.9 ps rise time) is limited to ca. d_{min} = 340 µm [11]. To demonstrate this in more detail, further CPS structures featuring defect structures with varying dimensions are investigated in a next step. The first DUT is sketched in Fig. 2(a). The comparison device is identical except for the distance between the gap and short discontinuity which is reduced from 100 µm to 50 µm.

Recorded time-transients are shown in Fig. 3. The transients demonstrate that this rather small changes of the distance can be clearly seen within the reflected signal. While the 100-µm-spaced gap/short defect structure still has the distinguishable second peak the 50-µm-spaced structure generates a characteristic signal shape without obvious second peak. However, the signal shape does neither match a single (open or short) fault but is a superposition of the two characteristic reflections. Therefore, the nearby discontinuities may be still identified through numerical signal analysis even though they are not obviously distinguishable in terms of separate peaks. Using knowledge of the characteristic signal-shapes from different types of discontinuities numerical calculations enable discrimination of discontinuities below the above given theoretical limits [10]. Hence the identification of fault combinations with distances as small as 20 µm is numerically feasible with the introduced technique.

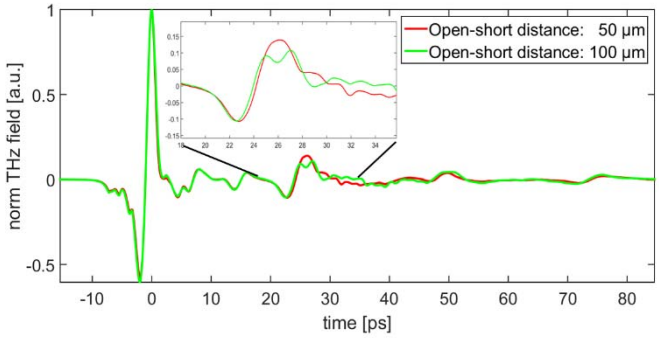

Fig. 3. Time-transients in reflection of two different DUTs similar to the one shown in Fig. 2(a). The DUTs only differ in distance of the half-open to short discontinuity.

In terms of facilitated handling the emitter and detector can be merged together into a single device. This does not only improve repeatability but also offers the ability to measure the reflection from the coupling of the transceiver structure to the DUT. Hence also insertion losses can be determined. Combining a transceiver at the beginning and a detector at the end of the DUT enables a full S-parameter analysis. Yet, such measurements have made use of horn antennas that had to be attached to the waveguide structures for the use of common THz free-space set-ups [12]. This again highlights the enormous advantage in terms of versatility and simplicity of the emitter and transceiver microprobes introduced in this work.

III. Summary

A novel emitter and transceiver microprobe set-up capable of injecting and measuring broadband THz signals of up to 2.5 THz and featuring rise times as short as 0.6 ps has been introduced. The performance has been demonstrated on coplanar stripline devices with closely spaced discontinuities highlighting the capability of complex propagation parameter measurement and highly resolving failure localization.

References

[1]. S. Laurette, A. Treizebre, A. Elagli et al., "Highly sensitive terahertz spectroscopy in microsystem," *RSC Advances*, 2, 10064–10071, 2012.

[2]. Y.-G. Kim, D.-S. Woo, K. W. Kim and Y.-K. Cho, "A New Ultra-wideband Microstrip-to-CPS Transition," *Microwave Symposium*, pp. 1563-1566, Honolulu, USA, June 3-8 2007.

[3]. Y. Kadoya, M. Onuma, S. Yanagi, T. Ohkubo, N. Sato and J. Kitagawa, "THz Wave Propagation on Strip Lines: Devices, Properties, and Applications," *Radioengineering,* 17(2), pp. 48-55, 2008

[4]. J. Shi, K. Kang, Y. Z. Xiong, F. Lin, "Investigation of CMOS on-chip transmission lines CPW, SCPW and CPWG up to 110GHz," *IEEE RFIT*, pp. 269-272, Singapore , 2009.

[5]. H.-M. Heiliger, M. Nagel, H. G. Roskos, et al., "Low-dispersion thin-film microstrip lines with cyclotene (benzocyclobutene) as dielectric medium," Appl. Phys. Lett. 70, 2233, 1997.

[6]. M. Nagel, P. H. Bolivar, M. Brucherseifer et al., "Integrated THz technology for label-free genetic diagnostics," Appl. Phys. Lett. 80, 154, 2002.

[7]. M. B. Byrne, J. Cunningham, K. Tych, A. D. Burnett, M. R. Stringer, C. D. Wood, L. Dazhang, M. Lachab, E. H. Linfield, and A. G. Davies, "Terahertz vibrational absorption spectroscopy using microstrip-line waveguides," Appl. Phys. Lett., 93, 182904, 2008.

[8]. M. Nagel, A. Michalski, H. Kurz, "Contact-free fault location and imaging with on-chip terahertz time-domain reflectometry," Opt. Express, 19(13), 12509-12514, 2011.

[9]. M. Martin, P.K. Daram, E.R. Brown, "Non-Contact Probes for Characterization of THz Devices and Components," *39th IRMMW*, Tucson, USA Sept. 14-19, 2014

[10]. E. McGibney, J. Barrett, "An Overview of Electrical Characterization Techniques and Theory for IC Packages and Interconnects," IEEE Trans. Adv. Packag., 29(1), pp. 131-139, 2006.

[11].Y. Cai, Z. Wang, R. Dias, and D. Goyal, "Electro optical terahertz pulse reflectometry - an innovative fault isolation tool," Electronic Components and Technology Conference (ECTC), 2010 Proceedings 60th, Las Vegas, NV, USA, 1309 – 1315, 2010.

[12]. J.-M. Rämer, G. v. Freymann, "A Terahertz Time-Domain Spectroscopy-Based Network Analyzer," J. Lightwave Technol., 33(2), pp.403-407, 2015.